Structural Identification of a Deteriorated Reinforced Concrete Bridge

Yun Zhou, Ph.D.[1]; John Prader, Ph.D.[2]; Jeffrey Weidner, Ph.D.[3]; Nathan Dubbs, Ph.D.[4]; Franklin Moon, Ph.D.[5]; and A. Emin Aktan, Ph.D.[6]

Abstract: Displacement coefficients and profiles have been proposed as objective indexes for bridge structural condition evaluation by many researchers. In this paper, experimental data of the following type were collected for structural identification (St-Id) of a deteriorated bridge: (1) static displacement and strain measurements taken under proof-load level and (2) multireference impact testing (MRIT) data from one of the spans of a three-span, cast-in-place reinforced concrete T-beam bridge (Smithers Bridge). The MRIT was used to generate the modal data for computation of the modal flexibility and displacement profiles. Several significant obstacles were encountered during the St-Id of the Smithers Bridge including high damping level (which led to difficulties in identifying and selecting the poles), finite-element (FE) model updating challenges, and correlation of the MRIT results with truck load test measurements. The first challenge was addressed through the use of the complex mode indicator function method of modal identification, which is capable of identifying highly damped modes. Then the updating of the FE model was accomplished using the *Strand7* FE analysis package coupled with the *MATLAB* application programming interface. Finally, to allow for direct comparison of the MRIT and truck load results, two strategies were employed. The first involved the redistribution of truck load force to the MRIT degrees of freedom and the second utilized interpolation functions for modal expansion of the MRIT results to include the truck tire locations. The St-Id procedure used during this application was designed to mitigate blatant human error and epistemic uncertainty in the data interpretation process. Successful results from the MRIT demonstrated the reliability of the applications for bridge condition assessment based on impact testing. **DOI: 10.1061/(ASCE)BE.1943-5592.0000309.**

CE Database subject headings: Concrete bridges; Deterioration; Assessment; Experimentation; Tests; Trucks; Load factors.

Author keywords: Bridge condition assessment; Structural identification (St-Id); Experimental modal analysis; Multiple-input multiple-output testing; Multireference impact testing (MRIT); Truck load testing; Model updating; Load rating.

Introduction

According to the Federal Highway Administration (FHwA 2011), more than 33% of the 604,485 bridges in the United States were built over 50 years ago, among which 43% are classified as either structurally deficient or functionally obsolete. To compound this problem, a significant portion of the bridge population lack documentation of their design details, as-constructed plans for foundation substructures and superstructures, and maintenance and repair records. In the absence of such information, estimates of the live load capacity and condition of bridges often depend solely on visual assessment, despite its substantial limitations and inherent subjectivity. Motivated by the need to provide additional tools to owners struggling to prioritize the rehabilitation or replacement of such bridges, the writers have been exploring strategies to augment current visual inspection procedures with an objective and reliable approach such as structural identification (St-Id) (Aktan et al. 1993, 1997, 1998).

The use of St-Id for condition evaluation will document the conditions of a bridge not in terms of a subjective integer but in terms of a comprehensive analytical model. This model should represent the three-dimensional (3D) geometry, boundary conditions, material characteristics such as concrete and steel stiffness, strength and their variations, as well as simulate the measured global mechanical properties such as frequencies, mode shapes, damping, and flexibility coefficients. Given the advances in computer hardware and software, bridge engineers should be able to unleash the power of finite-element (FE) analysis, and St-Id offers a disciplined and prudent way to do so. During the last 30 years, the state of the art in St-Id of constructed systems has advanced significantly and dozens of applications to many large and complex structural systems have been demonstrated (ASCE 2011). The ASCE Structural Identification of Constructed Systems Committee recommends the following six steps (ASCE 2011): (1) clearly defining the objectives for St-Id followed by observation and conceptualization of the entire structural-foundation-soil system by site visits and study of all legacy data/information, including sampling and testing materials; (2) a priori analytical modeling; (3) uncontrolled and/or controlled experiments; (4) processing and interpretation of data; (5) model-experiment correlation; and (6) utilization of the insight gained during Steps 1–5 in conjunction with the field-calibrated model for simulations and decision

[1]Associate Professor, College of Civil Engineering, Hunan Univ., Changsha, Hunan Province 410082, P.R. China; formerly, Postdoctoral Research Engineer, Drexel Univ., Philadelphia, PA 19104 (corresponding author). E-mail: zhouyun05@gmail.com

[2]Drexel Univ., Philadelphia, PA 19104. E-mail: jbp23@drexel.edu

[3]Drexel Univ., Philadelphia, PA 19104. E-mail: jsw24@drexel.edu

[4]Drexel Univ., Philadelphia, PA 19104. E-mail: ncd24@drexel.edu

[5]Associate Professor, Drexel Univ., Philadelphia, PA 19104. E-mail: FLM72@drexel.edu

[6]John Roebling Professor, Drexel Univ., Philadelphia, PA 19104. E-mail: aaktan@drexel.edu

Note. This manuscript was submitted on March 18, 2011; approved on September 14, 2011; published online on September 16, 2011. Discussion period open until February 1, 2013; separate discussions must be submitted for individual papers. This paper is part of the ***Journal of Bridge Engineering***, Vol. 17, No. 5, September 1, 2012. ©ASCE, ISSN 1084-0702/2012/5-774–787/$25.00.

making. Through these steps, bridge engineers may accomplish a true integration of experiment and analysis, as well as information technology and decision sciences.

Step 3 of St-Id may leverage controlled experiments such as static load applications, ambient monitoring, dynamic force applications, or a combination of these. Doebling et al. (1996, 1998) and Sohn et al. (2003) provide an overview of the vibration-based applications conducted during the previous 15 years while the state-of-the-art report by the ASCE Structural Identification of Constructed Systems Committee (ASCE 2011) provides an up-to-date description of the spectrum of experimental methods used in St-Id. Forced vibration testing (FVT) is a powerful method for experimenting with constructed systems and it is the only test method capable of providing an estimate of modal mass and modal flexibility. Various FVT methods include rotating eccentric mass exciters (Hudson 1964), electrodynamic shakers (Brownjohn et al. 2003), transient testing (Luscher et al. 2001), multireference impact testing (MRIT) (Autiabile 1998; Green and Cebon 1994; Reynders et al. 2010), and step relaxation (Gentile and Cabrera 1997).

Owing to its ease of application, MRIT, which was first developed in the 1970s (Halvorsen and Brown 1977), offers the greatest utility for bridge condition assessment because it may be executed relatively quickly. However, the primary challenge in its application is that aged and deteriorated highway bridges are often characterized by nonlinear behaviors that are often not observable, and these attributes violate the underlying assumptions of modal analysis. As a result, careful design and execution of the experiments and on-site validation of measurement quality and interpretation are required to understand the limits of a linear, stationary representation of the system.

Background, Motivations, and Objectives

In 2003 the state of West Virginia designated a Coal Resource Transportation System (CRTS) for coal trucks that are heavier than legal truck loads. The CRTS includes over 600 short-to-medium span bridge structures, many of which were constructed in the 1920s. A substantial portion of these older bridges are cast-in-place reinforced concrete (RC) slab, T-beam, and filled-arch bridges and their design and construction plans are missing. Their foundation characteristics are unknown and many of these bridges are structurally deficient and, therefore, posted based on inspectors' visual appraisal. This problem led to a joint research project between the Federal Highway Administration, the West Virginia Division of Highways, and Drexel University, and the writers were granted access to test several bridges throughout West Virginia. The writers performed St-Id on each type of bridge.

Successful MRIT was conducted on the HAM-42-0992 highway bridge (Aktan et al. 1997). The continuous, three-span steel-stringer Seymour Bridge (Catbas et al. 2006) was another earlier and successful demonstration of the application of MRIT for condition assessment, and excellent correlation was accomplished between the deflection profiles obtained from modal flexibility and the deflections measured under truck loads. This indicated the feasibility of using the truck load surface (TLS) from modal flexibility as a global condition indicator on a highway bridge. However, the Smithers Bridge as a cast-in-place RC test specimen represented a far more challenging nonsymmetric superstructure system with skew, and was covered by an asphalt overlay. There were no bearings at the interface between the superstructure and substructures and the details at the interface were unknown. There was extensive deterioration of the asphalt as well as the concrete deck under the asphalt. Owing to the much larger mass of the RC bridge and its widespread deterioration, whether it could be globally excited by an impact hammer was uncertain, and the quick decay of the response signals implied that this bridge may not lend itself to modal modeling. The high level of damping obscured successful identification of many of the poles in the frequency response functions (FRFs), biasing modal flexibility calculation. In addition, the redistribution of the truck loading owing to the opening of cracks caused large differences in the uniform load surface from modal flexibility and static test results, a phenomenon not observed previously Whether MRIT-based St-Id can be successful in the case of such a structure given its highly damped and closely coupled modes, was considered to be a highly challenging case to validate the applicability of MRIT as an experimental method as well as linearized St-Id itself. This is what motivated the writers to report their experiences with the Smithers Bridge. In this paper the bridge, both MRIT and proof-level-controlled truck-load tests, and each step in the St-Id procedure that was followed are described before presenting the conclusions and recommendations.

Description of the Smithers Bridge

The Smithers Bridge (Fig. 1) was a CTRS bridge constructed in 1930, located on Route 60 in Smithers, West Virginia. It is a three-span, simply supported RC T-beam bridge with 18° skew. Each span is approximately 14.40 m long, with a width (along the skew with sidewalk) of 14.63 m. There are six girders along each span with dimensions of 1.22×0.61 m (4×2 ft), with a transverse diaphragm along the width in the middle and on the downstream side of the span. Two additional partial diaphragms increase the stiffness and the mass on one side as shown in the plan in Fig. 1. The plans and reinforcing details did not exist for the structure; during the field inspection it was found that the beams sit on an unknown size bearing plate embedded in the pier cap. The bridge was posted by a consultant for 37 and 38 tons for two- and three-axle trucks, respectively. The posting impeded coal transportation and had negative impacts on the functionality of the regional transportation network. As a result, the West Virginia Department of Transportation (WVDOT) elected to have a load test and St-Id performed to more accurately assess the capacity and perhaps justify the removal of the posting.

The bridge exhibited deterioration in critical locations, including substantial spalling at the piers, pier caps, and beam seats. The beams exhibited flexural cracks and several shear cracks. In addition, the roadway surface showed substantial cracking at the piers and abutments. The bridge did not have any drainage system other than what was provided by a slight longitudinal elevation difference. Water and salt seeped through the joints between spans and created sediment buildup on the pier caps. Inspections indicated no signs of scour or other foundation-related problems.

Prior to the test, field measurements and material sampling informed the development of a priori FE models. Eleven steel samples were machined into ASTM 0.0127 m (0.5 in.) standard coupons and tested in tension. Seven 0.2286 m (9 in.) concrete cores were tested to reveal an average compressive strength of 5.34×10^7 N/m^2, with a standard deviation of 1.17×10^7 N/m^2. The modulus of elasticity of concrete was calculated based on the ACI code as 3.46×10^{10} N/m^2, to lie between 3.06×10^{10} and 3.82×10^{10} N/m^2 based on 95% confidence intervals. The elastic modulus of the rebar was confirmed as 2.0×10^{11} N/m^2.

Static Instrumentation

The a priori FE model was leveraged to design the instrumentation and load testing. The static instrumentation of the first span of the Smithers Bridge included 40 sensors to capture any opening or progression of the existing cracks, beam rebar strains, vertical

J. Bridge Eng. 2012.17:774-787.

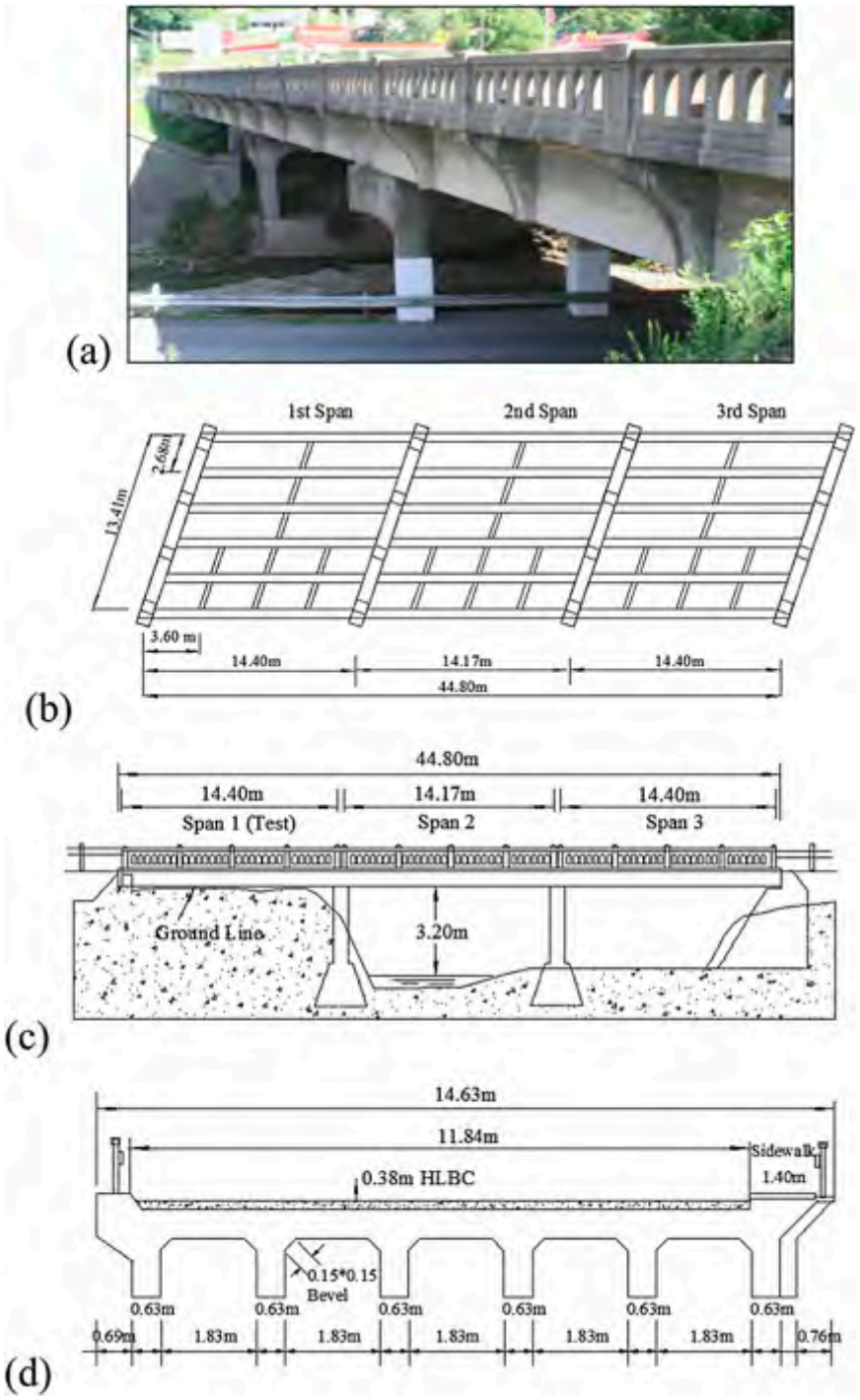

Fig. 1. Smithers Bridge: (a) photograph; (b) girder plan; (c) elevation; (d) cross section

displacements, and any settlements at the bearings. Because the first span was the most accessible span from the underside, a majority of the gauges were located under this span. The static instrumentation layout for the first span is shown in Fig. 2.

In the first span, cover concrete was chipped at 18 locations where strain gauges (Micro-Measurements Group) (Fig. 3) were microdot welded to beam reinforcing bars. Each gauge location was painted over to prevent any corrosion of the exposed steel, and these sensors provided a reliable measurement of the rebar strains. Twenty displacement transducers (Tokyo Sokki Kenkyujo, Co., Ltd.) (Fig. 3) were selected for measuring displacements. An additional three displacement transducers were installed to monitor any movements of the beam relative to the pier because the interface details between the beam and pier cap were unknown. A final displacement transducer was used to capture any lateral displacements of the pier cap. An OPTIM MegaDAC system was used for data acquisition and signal conditioning during the static tests. The OPTIM utilizes a 16-bit analog-to-digital converter. Data were logged at 20 Hz during the static tests.

Static Truck Load Test

The static load test was performed in 2008. The loads were applied using six special dump trucks capable of being loaded up to a total of

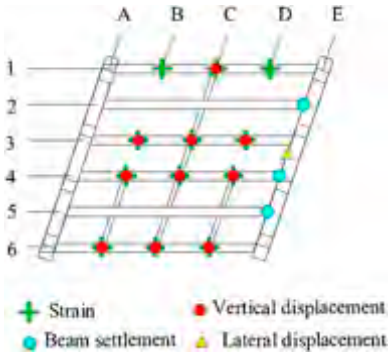

Fig. 2. Static instrumentation layout for the first span

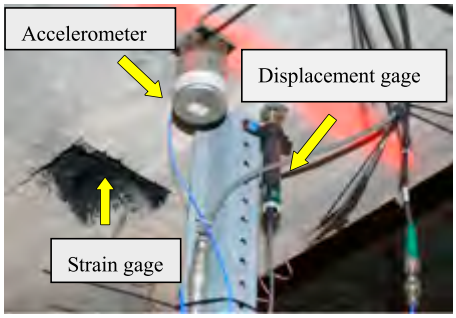

Fig. 3. Vertical displacement transducer, weldable strain gauge on steel rebar, and accelerometer

Fig. 4. Picture of six trucks during the load test

44.64 tons each. The National Cooperative Highway Research Program *Manual for Bridge Rating through Load Testing* (TRB 1998) indicated that for this structure and the state legal truck load of 40 tons, a proof load of 90 tons per lane or 268 tons total was required. The bridge was loaded incrementally from positioning three empty trucks to six fully loaded trucks for a total of 270 tons without any damage or distress. On average, each of the front-wheel tire loads were approximately 4.5 tons and the back-wheel tire loads were approximately 8.9 tons. The full load truck load test, shown in Fig. 4, resulted in excellent response levels, and the results for this test were used for parameter identification.

Based on the vertical displacement measurements, it was concluded that the continuity between spans was negligible because no deformation occurred in the span adjacent to the loaded span. The displacement response of the bridge was generally linear, with a small amount of softening. No significant nonlinearity was present in the global responses. The displacement profiles at 1/4, 1/2, and 3/4 points along the first span and under the full truck load is shown in Fig. 5. As expected, the largest response was at the midspan (−3.20 mm), with proportionally smaller responses at 1/4 and 3/4 spans. As a result of the skew, the response at 1/4 span is slightly larger than at 3/4 span. The maximum recorded steel strain was 150 microstrain at Axis c-4.

Modal Test by MRIT

In MRIT, the responses to a dynamic impact force are measured and the frequency response functions (FRFs) are computed to yield the modal parameters. In the case of systems that exhibit minor nonlinearity owing to distributed cracking, multireference testing in fact helps to rationally smear the nonlinearity into a linearized model. The unit-mass-normal modal coefficients obtained through such a test can be directly transformed to flexibility (Raghavendrachar and Aktan 1992). In the case of the Smithers Bridge, the impact was applied by an instrumented 11 kg PCB sledgehammer (Model 086D50, force <2,268 kg) with the medium plastic red polyurethane (Model 084A32) tip embedded in the impact head. The hammer is an easy-to-use versatile tool for conducting forced vibration testing. PCB 393C piezoelectric accelerometers (0.025–800 Hz, acceleration $< 2.5g$) were attached under the girders by magnetic mounts to steel plates firmly anchored into the concrete. An HBM 24-bit data acquisition system was used for data acquisition. A sampling frequency of 2,400 Hz was selected to capture the impact force at high resolution in the time domain. A dense modal grid was designed for the first span [Fig. 6(a)]. The hammer was used to

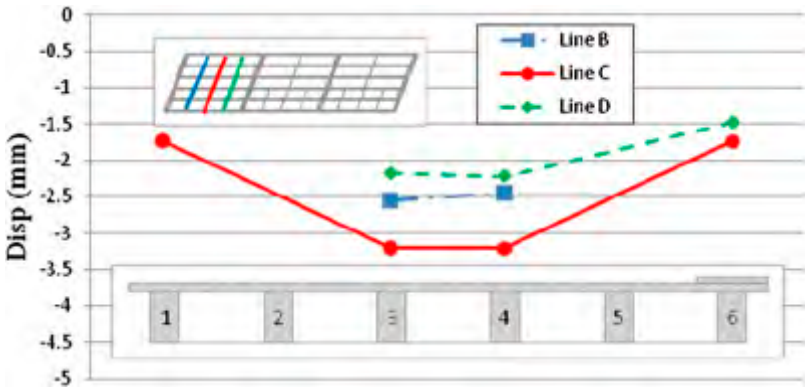

Fig. 5. Measured displacement results in the first span

J. Bridge Eng. 2012.17:774-787.

impact the roadway surface multiple times at six nodes (reference points) while the impact forces ranged from 15 to 22 kN. The six points shown in Fig. 6(a) were selected as the references. The typical hammer impact force and response signals in the time domain are shown in Fig. 7, while the reciprocity of the FRFs (accelerance) at Nodes 7 and 14 are shown in Fig. 8.

Ciloglu et al. (2012) presented the concept of an uncertainty path in operational modal analysis, showing that even proven and well-accepted data pre/postprocessing techniques may significantly bias modal analysis results when used in particular combinations. In this paper, the signals were preprocessed by using a rectangular-exponential window with 32,768 (2^{15}) fast Fourier transform points to provide a dense frequency resolution. A series of five impacts was conducted at each point and was used for calculation of the FRF. The H1 method (Ewins 1984) of estimating the modal parameters was used to extract the FRFs for further analysis with the complex mode indicator function (CMIF) (Shih et al. 1989; Phillips et al. 1998), stochastic system identification (SSI) (Peeters and De Roeck 1998, 2001; Peeters 2000), and PolyMAX (http://www.lmsintl.com) methods along a 60-Hz bandwidth.

The identified modal frequencies between 0 and 60 Hz are shown in Table 1, including the modal assurance criterion (MAC) values between the mode shapes calculated by two different methods. Mode shapes 1–6, 11, and 12 from all three methods correlate very well, with MAC values above 0.9. The bridge exhibits high damping, evident in Figs. 7 and 9. In Fig. 7 the response signal quickly decayed in 0.16–0.22 s, and the damping ratios in Table 1 identified by various modal analysis methods also reveal very high damping ratios exceeding 5% in many cases. High damping generally implies nonlinearity, as most constructed systems exhibit under 2% equivalent linear viscous damping at operational stress levels. MRIT exhibits all energy dissipation mechanisms as if they are all owing to linear proportional damping, and this leads to challenges in identifying the coupled modes as these are obscured in the singular value curves in Fig. 9. Filtering was omitted because it tends to flatten a FRF. The FRF (receptance) singular value curves produced by the CMIF method and shown in Fig. 9 include six curves for each of the reference points. The 12 modes that were selected between 0 and 60 Hz from the top curve were based on the location where a change in curvature existed. To establish whether the identified modes are true physical modes or just manifestations of the numerical analysis procedures, insight from FE simulations was necessary.

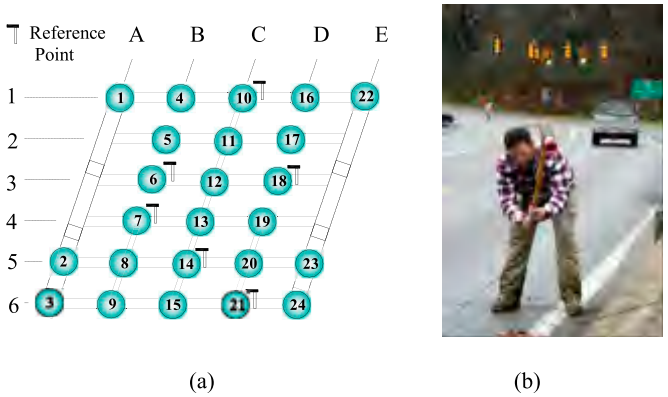

Fig. 6. (a) Dynamic instrumentation layout for the first span; (b) picture of on-site hammer impact testing

FE Model in *Strand7*

The FE model was constructed in *Strand7* (www.strand7.com), which is a commercially available FE software package. The measurements taken during the field visit in August 2008 were used to develop the FE models. The T-beam construction was modeled by a combination of frame, shell, and link elements. In total, the model consisted of 1,946 beam elements (including spring elements); 6,808 shell elements, 2,080 link elements, and 56,000 degrees of freedom (DOFs). As shown in Fig. 10, the model used frame elements to represent the beams, diaphragms, and piers of the structure, and the shell elements represented the deck. To simulate the composite action, the beams and the deck were connected using rigid links, which can be shown in Fig. 10, Details A and B. At the boundary locations, the beams were connected to the pier caps using lateral and vertical springs, with the moment released, which can be seen in Fig. 10, Detail C. Because the supports of the four piers were cast into a continuous concrete foundation, the support of the pier was set as a fixed boundary. The elastic modulus of the concrete for the entire structure was chosen as 3.46×10^{10} N/m^2, and this FE model was labeled as the initial model.

Based on a sensitivity analysis, the stiffness of the lateral and vertical springs simulating the bearings between the superstructure and the pier caps significantly influenced the eigenvalues of the FE model. By utilizing the vertical displacements measured at the beam ends and the lateral displacements of the pier cap, the spring stiffnesses were estimated from the test results, resulting in a boundary lateral spring stiffness of 4.55×10^8 N/m and a vertical spring stiffness of 1.92×10^7 N/m.

The static analysis of the FE model was conducted by using the measured tire weights for the six dump trucks. The tire loads were applied as point loads on the surface of the shell elements based on the

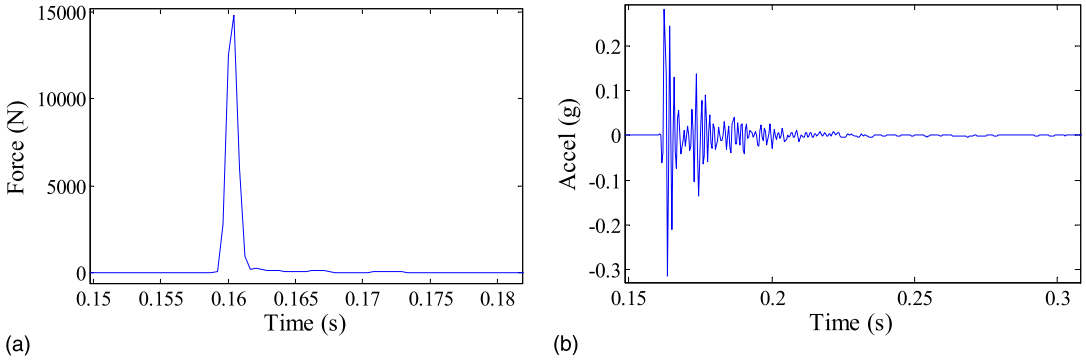

Fig. 7. (a) Typical hammer impact force in the time domain; (b) typical hammer response signal in the time domain (input at 7; output at 14)

J. Bridge Eng. 2012.17:774-787.

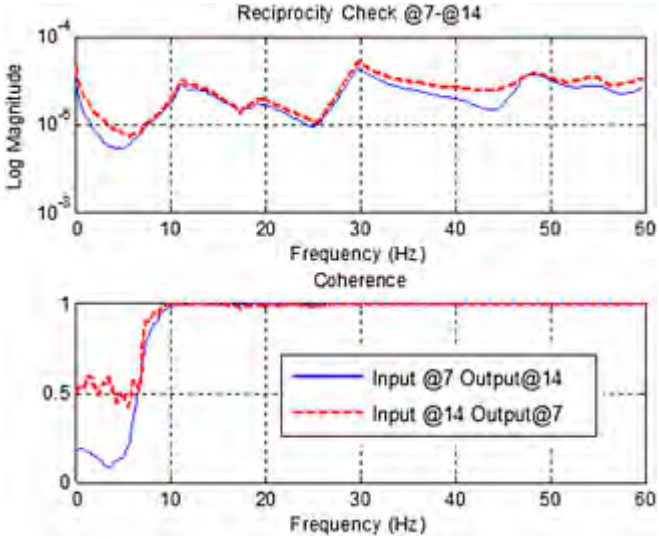

Fig. 8. Reciprocity check between various reference points

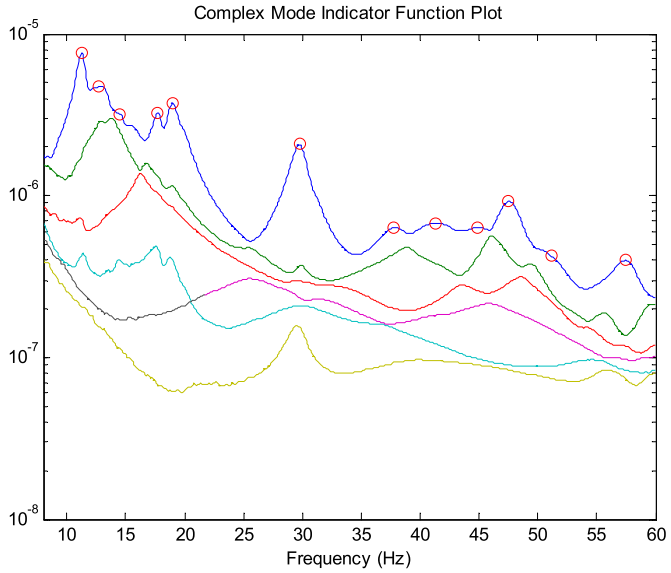

Fig. 9. Mode identification in the CMIF singular value curves

Table 1. Frequencies and Mode Shape MAC Comparisons from Various Algorithms

	CMIF		PolyMAX		SSI		MAC comparison		
Mode shape	Frequency (Hz)	Damping (%)	Frequency (Hz)	Damping (%)	Frequency (Hz)	Damping (%)	CMIF and PolyMAX	CMIF and SSI	PolyMAX and SSI
1	11.185	6.30	11.216	5.20	11.141	6.36	0.9799	0.9782	0.9801
2	12.952	13.33	13.033	7.35	12.988	7.08	0.9384	0.9916	0.9652
3	12.999	9.90	15.380	9.16	15.564	8.37	0.9490	0.9518	0.9963
4	18.074	7.28	17.676	2.72	17.538	3.91	0.9919	0.9804	0.9928
5	18.927	6.42	18.966	4.79	18.995	5.74	0.9981	0.9974	0.9993
6	29.707	2.69	29.697	2.92	29.669	3.05	0.9992	0.9979	0.9982
7	37.760	6.48	38.190	5.15	37.858	4.79	0.4531	0.9895	0.4752
8	40.848	8.48	39.779	11.21	—	—	0.8151	—	—
9	45.480	6.44	45.401	4.90	45.298	4.69	0.9510	0.9876	0.8993
10	47.608	2.59	47.773	5.96	47.576	2.73	0.8055	0.9907	0.7340
11	50.347	4.29	50.345	3.45	50.721	4.41	0.9902	0.9787	0.9933
12	57.586	2.76	57.476	2.62	57.617	2.50	0.9867	0.9801	0.9744

exact spacing of the truck tires, which was measured during the load tests. To accommodate this loading, the mesh at the deck was refined until it allowed simulating a very close approximation of the actual tire load locations. The measured displacement results from the first span were used as a baseline for comparison against the displacement profiles obtained by multiplying the modal flexibility matrix with a vector representing the truck loads applied during the static load test.

Modal Flexibility

Modal flexibility, which refers to a close approximation of flexibility extracted from modal test results, has been shown to be an excellent measure of flexibility if a sufficient number of modes are included (Clough and Penzien 1975). Modal flexibility has been proposed as a reliable experimental signature reflecting the existing condition of a bridge by Raghavendrachar and Aktan (1992) and can also serve as a stringent check to validate the accuracy and completeness of modal analysis results. There are two possible approaches for extracting modal flexibility, which are as follows: (1) the extraction of mass normalized mode shapes and modal frequencies, and (2) the identification of a synthesized FRF matrix, which was used in this study and is discussed subsequently.

Utilizing one of a number of available modal parameter estimation algorithms (Allemang and Brown 1998), a FRF between point p and q can be written as follows in the frequency domain as a partial fraction:

$$H_{pq}(\omega) = \sum_{r=1}^{m} \left[\frac{(A_{pq})_r}{j\omega - \lambda_r} + \frac{\left(A^*_{pq}\right)_r}{j\omega - \lambda^*_r} \right] \tag{1}$$

The residue term A_{pqr} can be expressed as $(A_{pq})_r = (\psi_{pr}\psi_{qr})/(M_A)_r$, and evaluating H_{pq} at $\omega = 0$ for DOFs p and q for modes r leads to the modal flexibility matrix. Substituting the previous expressions results in

$$H_{pq} = \sum_{r=1}^{m} \left[\frac{\psi_{pr}\psi_{qr}}{M_{A_r}(-\lambda_r)} + \frac{\psi^*_{pr}\psi^*_{qr}}{M^*_{A_r}(-\lambda^*_r)} \right] \tag{2}$$

where $H_{pq}(\omega)$ = FRF at point p owing to input at point q; A_{pqr} = residue for mode r; ω = frequency variable; λ_r = rth complex

J. Bridge Eng. 2012.17:774-787.

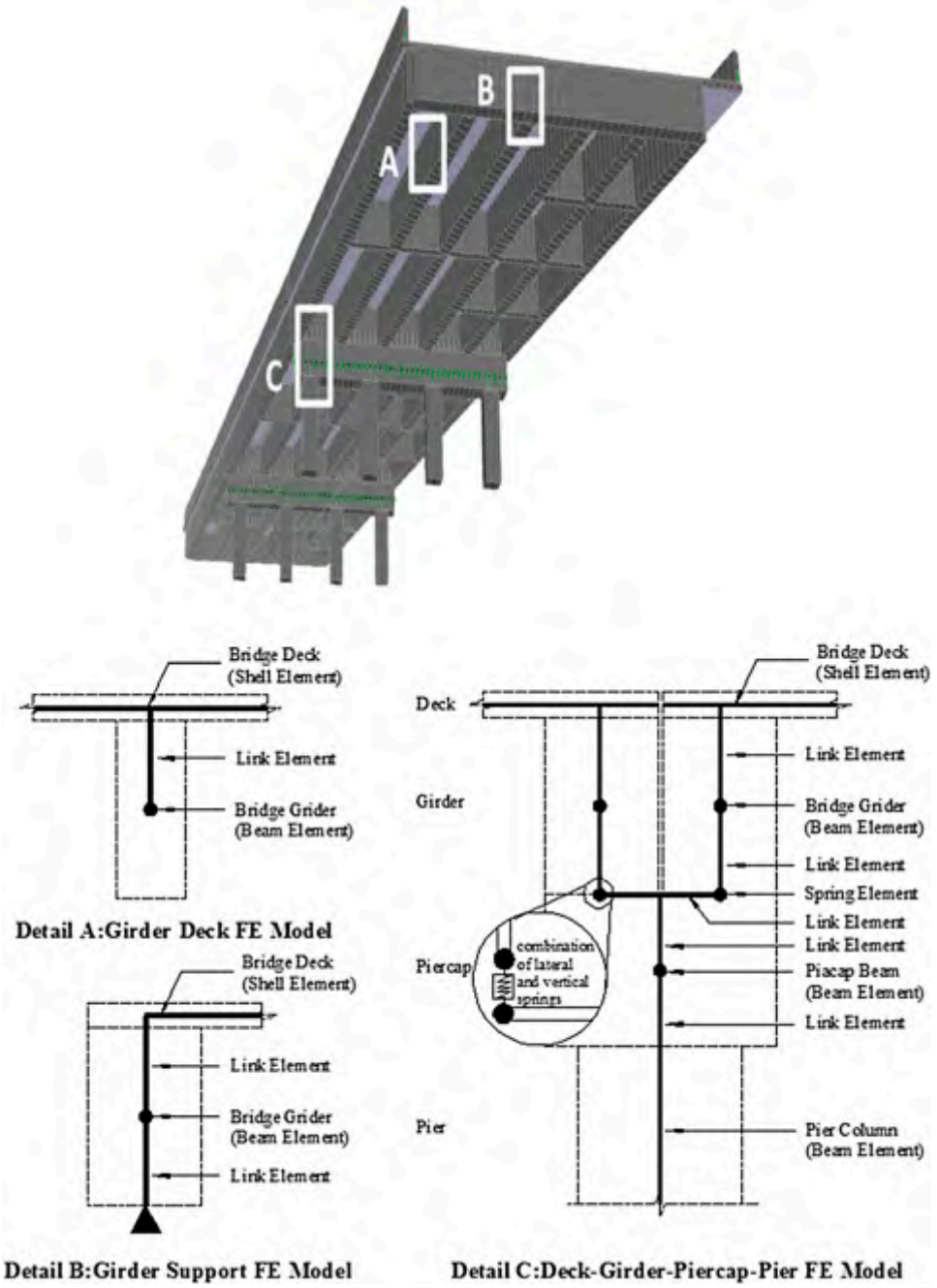

Fig. 10. FE model and simulation of the geometry

eigenvalue; ψ_p = mode shape coefficient at point p for the rth mode; and M_{Ar}= modal scaling for the rth mode. The flexibility matrix becomes

$$[f] = \begin{bmatrix} f_{11} = H_{11}(\omega = 0) & \cdots & f_{1q} = H_{1q}(\omega = 0) \\ \vdots & \ddots & \vdots \\ f_{p1} = H_{p1}(\omega = 0) & \cdots & f_{pq} = H_{pq}(\omega = 0) \end{bmatrix} \quad (3)$$

This flexibility matrix is an approximation of the static flexibility matrix because of modal truncation. Generally, the lower modes contribute substantially to modal flexibility, and when appropriate numbers of tested modes are identified the discrepancy between modal and static flexibility becomes negligible.

Modal Flexibility Calculation for the Smithers Bridge

The modes identified by the CMIF method were chosen to calculate the modal flexibility. In the modal grid, 24 nodes with accelerometers were distributed on the first span as shown in Fig. 6(a). In this instrumentation layout, the responses at six of the boundary points were not measured owing to instrumentation limitations and these boundary nodes were assumed to have zero response. A different challenge involved the loading of the flexibility matrix using the actual tire loads applied during the static load test. The load test was executed by six trucks with 36 tire loads. During the load test it was not possible to position the 36 truck tire positions to precisely correspond to the modal grid. This presented a challenge in correlating the static deflections with those obtained through modal flexibility. The subsequent

sections discuss the measures taken to correlate the deflection basins from static measurements and simulated by modal flexibility.

Strategy 1: Redistribution of the Truck Loads

One strategy of redistributing the truck loads is to use the measured mode shapes (each mode includes 24 coordinates) and the estimated modal mass to calculate modal flexibility, resulting in a 24 × 24 modal flexibility matrix corresponding to each node of the measurement grid. The truck tire positions do not match the measured node position as shown in Fig. 11(a); therefore, the loads have to be transformed to the instrumentation points as static equivalent loads as shown in Fig. 11(b). By using this method, a 1 × 24 load vector can be developed to coincide with the 24 measurement coordinates, and it can be used to multiply the 24 × 24 modal flexibility matrix, which results in the TLS.

In extracting modal flexibility from multiple-input multiple-output test results, the first 12 modes were used. A modal flexibility to static flexibility convergence analysis for the modal grid points on Girders 3, 4, and 6 were performed as shown in Fig. 12. The study indicated that the first five modes were essentially sufficient for convergence. The first five modes were between 10 and 20 Hz as shown in Table 1, and the remainder of the identified modes started at nearly 30 Hz. The higher modes had decreasing contributions to flexibility because the contribution of each mode was proportional to $1/\omega^2$. The small differences between the measured deflection and the calculated TLS by using modal flexibility ranged between 6.53 and 19.26% (Table 2) and these may be a result of various error sources. The question was how much of these discrepancies may be attributed to the transformation of truck tire locations to the instrumentation locations. Because the deck was skewed and had unsymmetric mass and stiffness distributions, unsymmetric modes had various contributions to the TLS. For example, in Fig. 12(c), the first mode brings TLS close to the load test results; however, after adding the second mode the flexibility starts to diverge from the truck load test results. After adding additional modes, the TLS begins to converge back to the static truck load test results.

FE Model Calibration

The *Strand7* software, through an application programming interface (API), interfaces with *MATLAB* to make use of the many toolboxes available (statistical, optimization, etc.) for updating FE models. The API can be used to create, read, and modify *Strand7* FE model data; launch the solvers; and extract results. After integration of the general coding strategy with the specific internal function from *Strand7*, the model calibration process can be run automatically.

Under the six truck load test, the tensile strain in the RC beams exceeded the strain at which cracking begins. The beams exhibited substantial cracking, especially in the middle portion of the bridge. As a result, the parameter identification was carried out using six average crack-height parameters y, corresponding to the six primary girders. As shown in Fig. 13(a), the rectangular girders have dimensions of 1.22 × 0.61 m (48 × 24 in.), and are reinforced with five Number 11 bars. The transformed section properties are calculated with the neutral axis at 0.63 m (24.67 in.) from the upper boundary of the beam, and the ratio of the moment of inertia of the transformed section to the original section is about 1.08 [in Fig. 13(b)]. The crack height, y, is defined as shown in Fig. 13(c). After cracking has begun, the effective compressive area is shaded. It is assumed the loading is such that the concrete compressive stress never exceeds $0.5f_c'$ and the steel does not yield. Both materials continue to behave elastically; therefore, the compressive stress distribution can be approximated as a triangle. The moment of inertia and compressive area are recalculated and used here to define two parameters, the ratio for stiffness (RI) in Eq. (4) and the ratio for area (RA) in Eq. (5). Both the RA and RI will decrease with an increase of y, as shown in Fig. 14

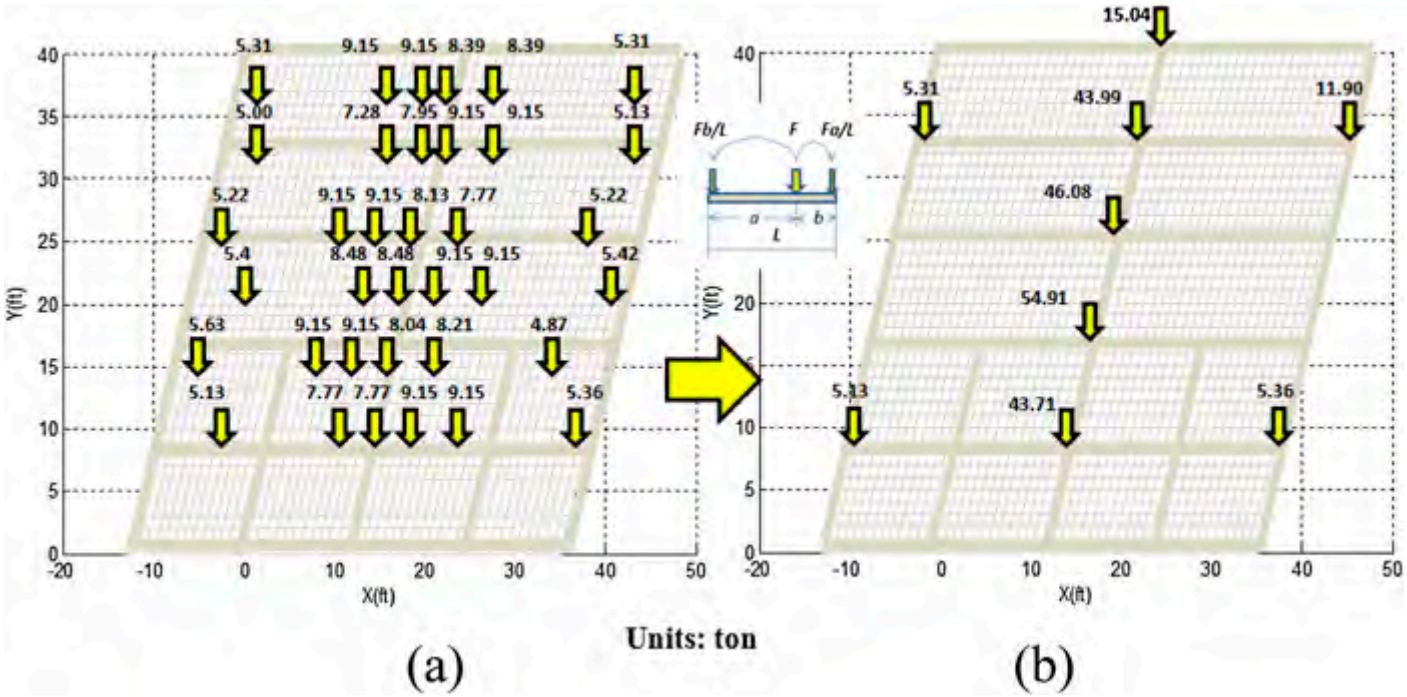

Fig. 11. Redistribution of the truck load for Strategy 1: (a) original load pattern; (b) redistributed load pattern

J. Bridge Eng. 2012.17:774-787.

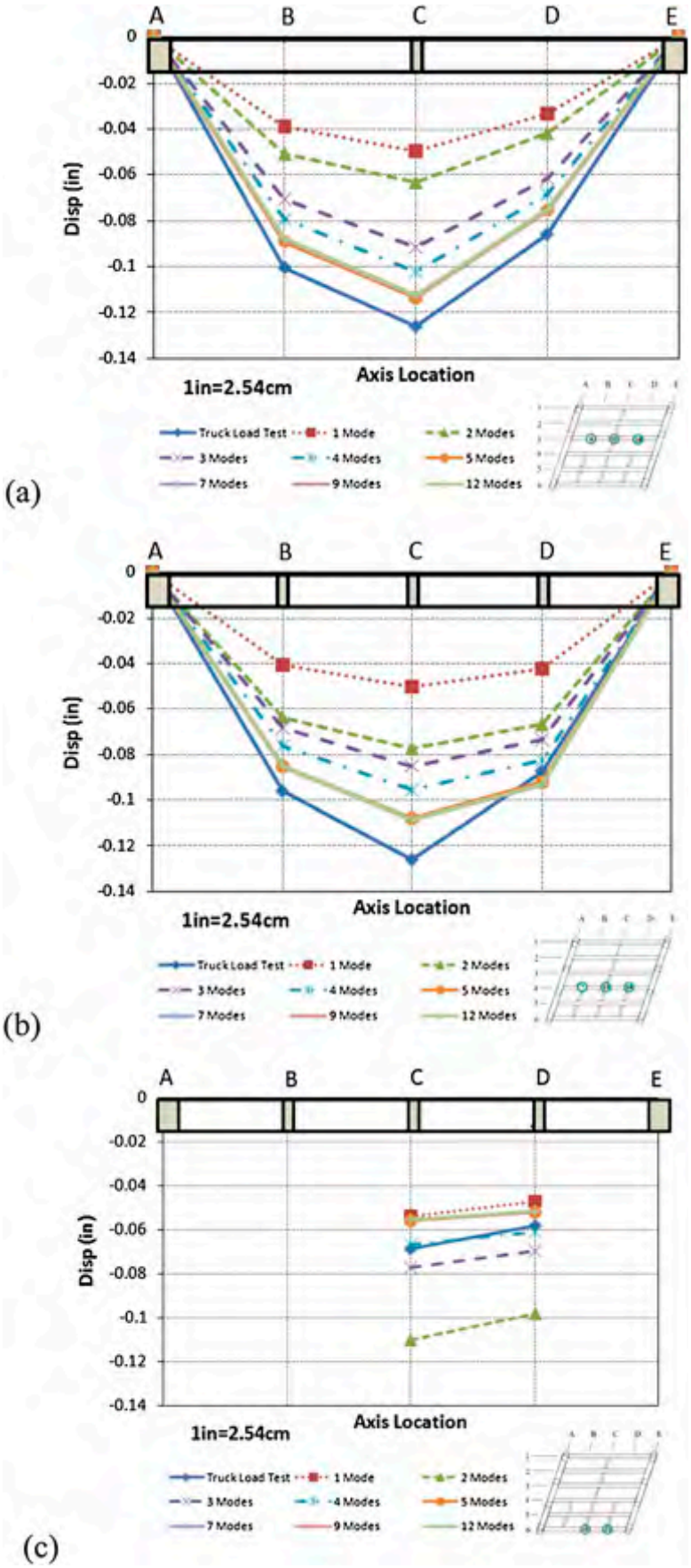

Fig. 12. TLS convergence study deflections in Strategy 1: (a) Girder 3; (b) Girder 4; (c) Girder 6

J. Bridge Eng. 2012.17:774-787.

$$\text{RI} = \frac{I_{\text{trans\_after\_crack}}}{I_{\text{trans\_before\_crack}}} \tag{4}$$

$$\text{RA} = \frac{A_{\text{trans\_after\_crack}}}{A_{\text{trans\_before\_crack}}} \tag{5}$$

In the parameter identification process, the average crack heights for the middle portion of the six primary girders were selected as the six updatable parameters to be used to calibrate the Smithers Bridge FE model using modal data as shown in Fig. 15. The selected area identified for updating was based on observations made in the field and moment diagram analysis performed on the preliminary FE model.

The measured frequencies and mode shapes were used for model calibration. The objective function to be minimized is the combined error of modal data between analysis (denoted as "ana") and experiment (denoted as "exp"), expressed as

$$J(p) = \sum_{i=1}^{n} \left[\frac{f_i^{\text{exp}} - f_i^{\text{ana}}(p)}{f_i^{\text{exp}}(p)} \right]^2 + \sum_{i=1}^{n} [1 - \text{MAC}_i(p)]^2 \tag{6}$$

$$\text{MAC}_i = \frac{\left(\phi_{\text{exp},i}^T \phi_{\text{ana},i}\right)^2}{\left(\phi_{\text{exp},i}^T \phi_{\text{exp},i}\right)\left(\phi_{\text{ana},i}^T \phi_{\text{ana},i}\right)} \tag{7}$$

where p = vector of the structural parameters to be updated, $f_i = i$th eigenvalue, $\phi_i = i$th mode shape, and $\text{MAC}_i = i$th mode MAC value. The nonlinear least-squares curve fitting function lsqnonlin in the *MATLAB* optimization toolbox was utilized for parameter updating analysis. The elastic modulus was defined as 5.34×10^7 N/m^2 for the global structure and held constant during the calibration procedure. The identified average crack heights following calibration are shown in Table 3.

The *Strand7* API was also used to extract the mode shape component from the 2,008 FE node points from the deck of the first span for each mode. After the model calibration procedure, the 12 calculated frequencies closely approximated the measured frequencies with a maximum relative error of 5.69% and an average relative error of 2.40%. In the case of the mode shapes, the correlation was not as successful as with the correlation of frequencies. The first through fifth and seventh and eighth mode shapes had higher MAC values (generally, above 0.8) while the ninth through 12th modes had lower MAC values, perhaps because the cubic interpolation functions proved too coarse for these higher modes. The writers noted the modes that had lower MAC values had less influence on the modal flexibility, as discussed in relation to the modal flexibility convergence study presented in Strategy 1. The 12 identified modes after interpolation using the cubic interpolation method are shown in Fig. 16 in 3D view.

Table 2. Percentage Error between the Measured Deflection and Calculated TLS by Strategy 1

Point number	6	12	18	7	13	19	15	21
Error (%)	12.74	10.66	12.75	11.33	13.97	6.53	19.26	11.24

Note: Error(%) $= |U_{\text{cal}} - U_{\text{mea}}|/U_{\text{mea}} \times 100\%$, where U_{cal} = calculated TLS by using 12 modes and U_{mea} = measured deflection.

Strategy 2: Utilizing the Expanded Mode Shapes

To understand the impacts of transforming static load positions for correlating the deflection from static and dynamic tests, a second strategy was formulated based on modal expansion. In this strategy, the two-dimensional cubic interpolation function interp2 in the *MATLAB* software was utilized for modal expansion of the 24 instrumentation coordinates into 2,008 analytical coordinates. Expanded mode shapes enabled the calculation of a larger order modal flexibility such that the coordinates of the modal flexibility coincided with the truck tire positions in the load test. Then, the TLS from the modal flexibility could be directly correlated with the measured displacements.

The correlations between the displacements obtained from the static load test and from the modal flexibility that was based on modal expansion are shown in Fig. 17. The TLS from the higher-order modal flexibility moved closer to the displacement profiles measured from the static truck load test and the average discrepancy was reduced from 11.33 to 3.14% for the internal girder and from 15.25 to 10.19% for the external girder, as shown in Table 4. The two nodes with larger errors lie along the edge beam, pointing to the magnitude of uncertainty that is inevitable in static or dynamic testing and the St-Id of large constructed systems in the field, and also implying the additional challenges in MRIT of deteriorated concrete structures with skew, unsymmetric mass, and stiffness properties.

The measured frequencies and mode shapes were used for FE model calibration as discussed previously, and the FE model was used for calculating the bridge load rating factors. Load ratings were calculated for the Smithers Bridge at both inventory and operating levels using the LRFR manual (AASHTO 2003). The calibrated model was used to calculate updated load ratings based on the 40-ton state legal truck load for which the bridge is posted. The load rating is for flexure of the beams, and is based on the worst case demand, calculated using a moving load on the calibrated model.

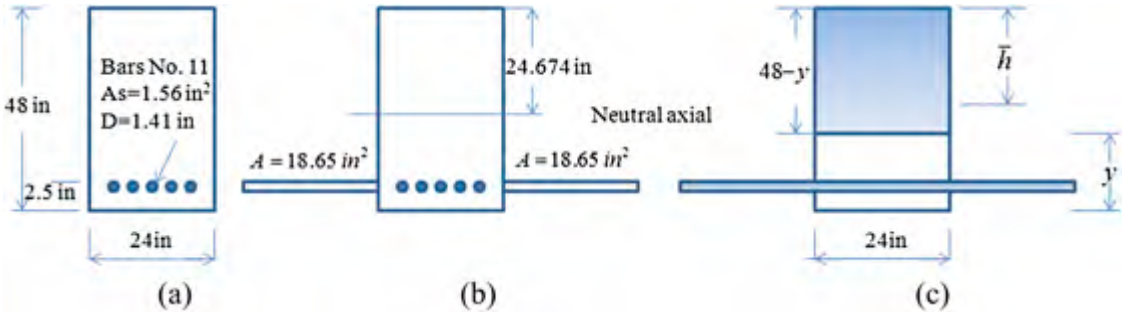

Fig. 13. Girder section properties before and after the crack appears (1 in. = 25.4 mm): (a) original section; (b) transformed section before the crack; (c) transformed section after the crack

J. Bridge Eng. 2012.17:774-787.

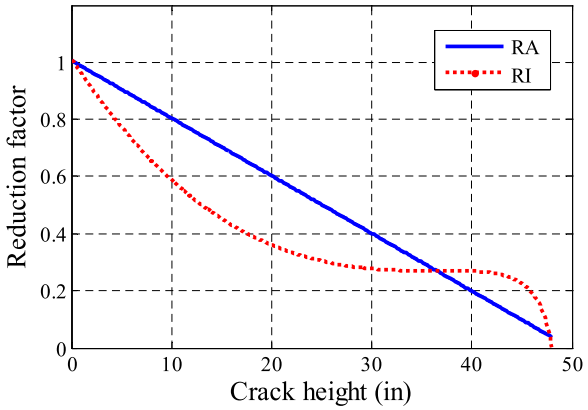

Fig. 14. Relationship of RI and RA with average crack height y (1 in. = 25.4 mm)

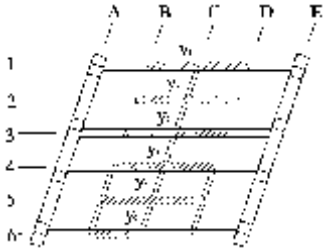

Fig. 15. Assumed updating area using the average crack height

Table 3. Identified Average Crack Height after Model Calibration

Parameter	Girder 1	Girder 2	Girder 3	Girder 4	Girder 5	Girder 6
y (mm)	74.92	123.38	318.42	380.80	219.24	88.80
RI	0.8648	0.7792	0.5138	0.4532	0.6336	0.8394
RA	0.9470	0.9085	0.7536	0.7040	0.8324	0.9360

The inventory and operating factors were equal to 3.64 and 2.87, respectively, which were both greater than 1. It indicated that with minor cosmetic repair, the posting of the bridge may be safely removed to permit the bridge to serve coal trucks.

Discussion and General Conclusions

This paper demonstrated how the writers leveraged St-Id for objective condition assessment and load capacity rating of an 80-year-old deteriorated, cast-in-place RC bridge that lacked design or construction plans and was posted. To perform St-Id reliably at full operating stress levels, the bridge was loaded by proof-level loads and over 40 displacement and strain responses were captured. In addition, a dynamic impact test was performed to evaluate the validity of the modal analysis on this bridge with an uncommon, highly unsymmetric distribution of mass and stiffness in addition to skew.

The challenges in each of the six steps of St-Id are discussed, and the results were validated by correlating measured and simulated deflections as well as measured and simulated frequencies and mode shapes. Having two independent sets of experiments—both static and dynamic—was useful for validating the reliability of the experimental results as well as the analytical model. The discrepancies between the measured and simulated displacements (10 displacements were measured under the loaded span in the truck load test) and the frequencies (12 frequencies were captured in the dynamic test) generally remained less than 5%, while the largest discrepancy remained under 15%. The MAC values for the first six measured and simulated mode shapes were above 0.9.

This level of correlation is sufficient to inspire confidence in the calibrated FE model as an acceptable representation of the global behaviors of the bridge. This model, although neither unique nor reliable for all local responses, may serve as a vehicle for load rating, failure-mode analysis, retrofit design, and other common concerns in relation to aged and deteriorated constructed systems. However, this model should not be used to predict the specific local responses of the bridge under loads, or for any decision that requires over 80% confidence in the simulated responses. Therefore, the model can only be useful under the supervision of an experienced engineer, and can never be a substitute for sound heuristic knowledge. Unfortunately, there are very few university laboratories, government agencies, and civil engineering consultants with the experience, capacity, and tools to perform the St-Id of a constructed system, especially when the system is deteriorated.

In spite of a lack of expertise for St-Id in the current practice of bridge engineering, the writers believe that by having more academic programs emphasize this concept, while the existing community of St-Id experts continue to accumulate example applications demonstrating best practices, and by relying on advances in intelligent software and hardware, it is possible to envision an industry capable of practical and reliable St-Id applications in a decade or two.

It is important to note that if the writers had not performed a proof-level load test while measuring over three dozen local and global responses of one span of the bridge, they would not be able to recommend removing the bridge posting. On the other hand, if the writers had performed the proof-level test without such dense measurement, and had not calibrated a FE model for rating the bridge, they still would not have been able to recommend removing the bridge posting. It is concluded that just the experimental components of St-Id are not sufficient for decision making. Only by integrating heuristic knowledge, experiment, analysis, and infrastructure decision-making principles such as uncertainty, risk, lifecycle benefit/cost, and sustainability can it be expected that reliable St-Id for use in infrastructure will be accomplished.

Specific Conclusions

The application described in the paper demonstrated that MRIT can be successfully applied to generate a linear modal characterization of a deteriorated bridge with widespread cracking. Some specific conclusions are drawn in the following:

1. The applied dynamic test data postprocessing techniques were selected to bound and reduce the epistemic uncertainty in identifying the modal properties, especially FRF selection, modal data validation, and mode shape expansion. The results of the two different strategies to correlate the modal flexibility and measured TLSs indicated that in the case of deteriorated and cracked bridges, certain common data interpretation procedures may significantly bias the final condition assessment results.
2. A dense instrumentation grid and many reference nodes become important for a complicated structure such as the Smithers Bridge, especially when the modal density in the lower-frequency bandwidth is high and the structure exhibits high damping for most modes. Coupled bending and torsional modes exist owing to the nonsymmetric geometry and mass; these would not be possible to capture with just an array along a sidewalk or sparse instrumentation.

J. Bridge Eng. 2012.17:774-787.

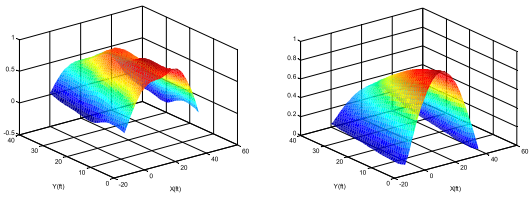

f_{1st_FE} =11.564 Hz (Δf=3.28%, MAC_{1st} =0.9763)

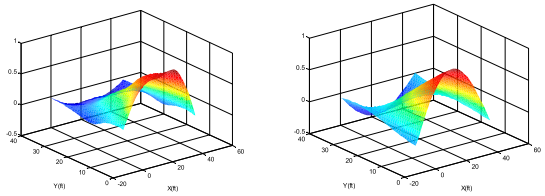

f_{2nd_FE} = 12.970 Hz (Δf=0.14%, MAC_{2nd} =0.9621)

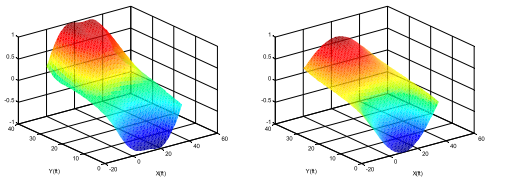

f_{3rd_FE}= 13.784 Hz (Δf=5.69%, MAC_{3rd} =0.9663)

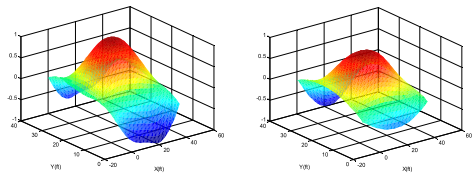

f_{4th_FE}= 19.153 Hz (Δf=5.63%, MAC_{4th} =0.9497)

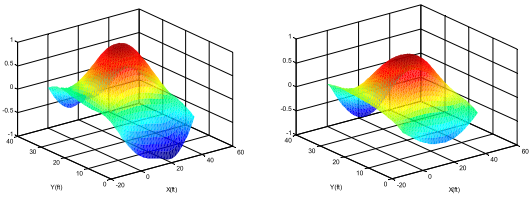

f_{5th_FE}= 19.397 Hz (Δf=2.42%, MAC_{5th} =0.9614)

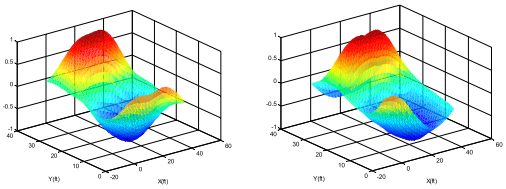

f_{6th_FE}= 31.319 Hz (Δf=5.15%, MAC_{6th} =0.7184)

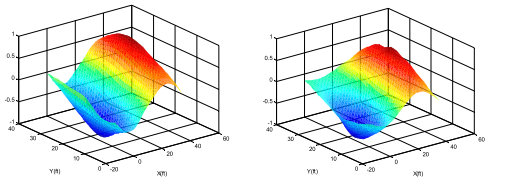

f_{7th_FE}= 38.294 Hz (Δf=1.39%, MAC_{7th} =0.8300)

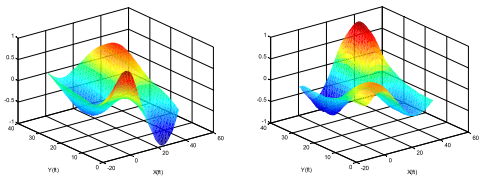

f_{8th_FE}= 40.637 Hz (Δf=0.52%, MAC_{8th} =0.9310)

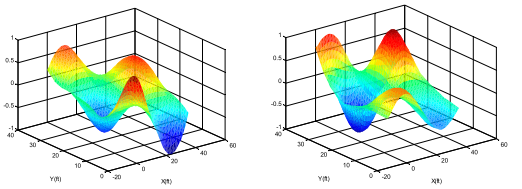

f_{9th_FE}= 45.393 Hz (Δf=0.19%, MAC_{9th} =0.4885)

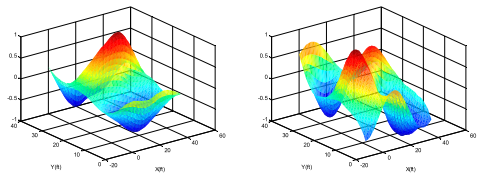

f_{10th_FE}= 46.682 Hz (Δf=1.98%, MAC_{10th} =0.6304)

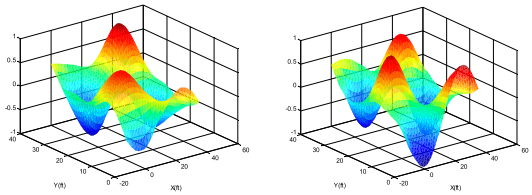

f_{11th_FE}= 51.192 Hz (Δf=1.34%, MAC_{11th} =0.4731)

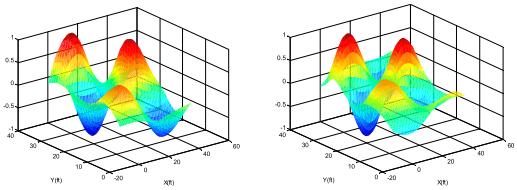

f_{12th_FE}= 58.192 Hz (Δf=1.04%, MAC_{12th} =0.5608)

Fig. 16. Comparison of the interpolated modes by measurement and calculated modes by the FE model

J. Bridge Eng. 2012.17:774-787.

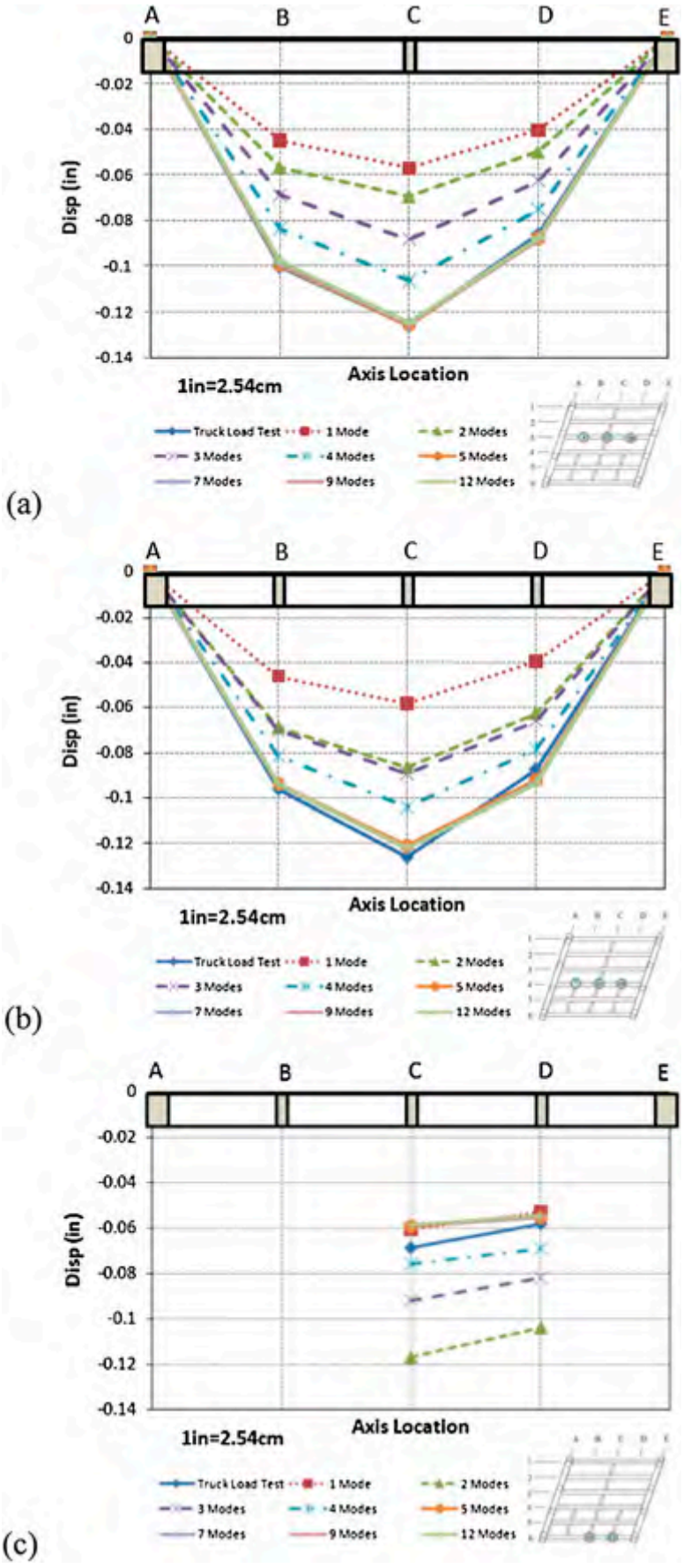

Fig. 17. TLS convergence study of deflections in Strategy 2: (a) Girder 3; (b) Girder 4; (c) Girder 6

J. Bridge Eng. 2012.17:774-787.

Table 4. Percentage Error between the Measured Deflection and Calculated TLS by Strategy 2

Point number	6	12	18	7	13	19	15	21
Error (%)	2.39	1.07	2.38	2.60	3.32	7.08	14.48	5.89

Note: Error(%) $= |U_{cal} - U_{mea}|/U_{mea} \times 100\%$, where U_{cal} = calculated TLS by using 12 modes and U_{mea} = measured deflection.

3. Based on the study, the CMIF and PolyMAX methods showed advantages over the SSI method, which is based on the time-domain identification. The CMIF is a powerful tool that can be used to facilitate peak picking based on the curvature changes in the FRF to identify a mode, in addition to providing accurate modal mass.
4. Two different strategies to redistribute the truck load on the bridge deck for analysis have been demonstrated. A condensation of truck loads based on static equivalency to match instrumentation points produced larger errors in the estimation of the TLS. The mode shape interpolation procedure reduced these errors by allowing the truck loads to be distributed spatially in a similar manner as to the distribution observed during the load test.

Acknowledgments

The writers express their deep appreciation to their colleagues at the Federal Highway Administration and Turner-Fairbanks Highway Research Center, especially to the former Chief Science Officer of the FHwA, Dr. Steven Chase, for their confidence and support. The writers are grateful for the contributions made by Dr. Frank Jalinoos, Director of the NDE Center, and Dr. Hamid Ghasemi, Manager of the Long-Term Bridge Performance Program. The West Virginia Department of Transportation has made major contributions to this research. From the outset, the writers had the opportunity to work closely with Frank Liss and John Taylor as well as several district engineers and their staff. The WVDOT engineers who participated in this research were instrumental in the success of the research and the writers are indebted to them for their efforts.

References

AASHTO. (2003). *Guide manual for condition evaluation and load and resistance factor rating (LRFR) of highway bridges*, AASHTO, Washington, DC.

Aktan, A. E., et al. (1997). "Structural identification for condition assessment: Experimental arts." *J. Struct. Eng.*, 123(12), 1674–1684.

Aktan, A. E., Catbas, N., Turer, A., and Zhang, Z. F. (1998). "Structural identification: Analytical aspects." *J. Struct. Eng.*, 124(7), 817–829.

Aktan, A. E., Chuntavan, C., Toksoy, T., and Lee, K. L. (1993). "Structural identification of a steel-stringer bridge for nondestructive evaluation." *Transportation Research Record 1393*, National Research Council, Transportation Research Board, Washington, DC, 175–185.

Allemang, R. J., and Brown, D. L. (1998). "A unified polynomial approach to modal identification." *J. Sound Vib.*, 211(3), 301–322.

ASCE. (2011). "Structural identification of constructed systems." *ASCE-SEI Structural Identification of Constructed Systems Committee State-of-the-Art Rep.*, ASCE, Reston, VA.

Autiabile, P. (1998). "Modal space-back to basics: Is there any difference between a roving hammer and roving accelerometer test." *Exp. Tech.*, 22(5), 9–10.

Brownjohn, J. M. W., Moyo, P., Omenzetter, P., and Lu, Y. (2003). "Assessment of highway bridge upgrading by dynamics testing and finite element model updating." *J. Bridge Eng.*, 8(3), 162–172.

Catbas, F. N., Brown, D. L., and Aktan, A. E. (2006). "Use of modal flexibility for damage detection and condition assessment: Case studies and demonstrations on large structures." *J. Struct. Eng.*, 132(11), 1699–1712.

Ciloglu, K., Zhou, Y., Moon, F., and Aktan, A. E. (2012). "Impacts of epistemic uncertainty in operational modal analysis." *J. Eng. Mech.*, 10.1061/(ASCE)EM.1943-7889.0000413 (Feb. 13, 2012).

Clough, R., and Penzien, J. (1975). *Dynamics of structures*, McGraw-Hill, New York.

Doebling, S. W., Farrar, C. R., and Prime, M. B. (1998). "A summary review of vibration-based damage identification methods." *Shock Vib. Dig.*, 30(2), 91–105.

Doebling, S. W., Farrar, C. R., Prime, M. B., and Shevitz, D. W. (1996). "Damage identification and health monitoring of structural and mechanical systems from changes in their vibration characteristics: A literature review." *Rep. LA-13070-MS,* Los Alamos National Laboratory, Los Alamos, NM.

Ewins, D. J. (1984). *Modal testing: Theory and practice*, Wiley, New York.

Federal Highway Administration (FHwA). (2011). *National bridge inventory*, U.S. Dept. of Transportation, FHwA, Washington, DC.

Gentile, C., and Cabrera, F. (1997). "Dynamic investigation of a repaired cable-stayed bridge." *Earthquake Eng. Struct. Dyn.*, 26(1), 41–59.

Green, M. F., and Cebon, D. (1994). "Dynamic response of highway bridges to heavy vehicle loads: Theory and experimental validation." *J. Sound Vib.*, 170(1), 51–78.

Halvorsen, W. G., and Brown, D. L. (1977). "Impulse technique for structural frequency response testing." *J. Sound Vib.*, 11(11), 8–21.

Hudson, D. E. (1964). "Response testing of full-scale structures." *J. Engrg. Mech. Div.*, 90(3), 1–9.

Luscher, D. L., Brownjohn, J. M. W., Sohn, H., and Farrar, C. (2001). "Modal parameter extraction of Z24 bridge data." *Proc., 19th Int. Modal Analysis Conf.*, Kissimmee, FL, Society of Experimental Mechanics, Bethel, CT, 836–841.

Peeters, B. (2000). "System identification and damage detection in civil engineering." Ph.D. thesis, Katholieke Univ., Leuven, Belgium.

Peeters, B., and De Roeck, G. (1998). "Stochastic subspace system identification of a steel transmitter mast." *Proc., 16th Int. Modal Analysis Conf.*, Society for Experimental Mechanics, Bethel, CT, 130–135.

Peeters, B., and De Roeck, G. (2001). "Stochastic system identification for operational modal analysis: A review." *J. Dyn. Syst. Meas. Control*, 123(4), 659–667.

Phillips, A. W., Allemeng, R. J., and Fladung, W. A. (1998). "The complex mode indicator function (CMIF) as a parameter estimation method." *Proc., 16th Int. Modal Analysis Conf.*, Society for Experimental Mechanics, Bethel, CT, 705–1041.

Raghavendrachar, M., and Aktan, A. E. (1992). "Flexibility by multi-reference impact testing for bridge diagnostics." *J. Struct. Eng.*, 118(8), 2186–2203.

Reynders, E., Degrauwe, D., De Roeck, G. D., Magalhaes, F., and Caetano, E. (2010). "Combined experimental-operational modal testing of footbridges." *J. Eng. Mech.*, 136(6), 687–696.

Shih, C. Y., Tsuei, Y. G., Allemang, R. J., and Brown, D. L. (1989). "Complex mode indication function and its applications to spatial domain parameter estimation." *Proc., 7th Int. Modal Analysis Conf.*, Society for Experimental Mechanics, Bethel, CT, 533–540.

Sohn, H., et al. (2003). "A review of structural health monitoring literature: 1996–2001." *Rep. LA-13976-MS*, Los Alamos National Laboratory, Los Alamos, NM.

Transportation Research Board of the National Academies (TRB). (1998). *Manual for bridge rating through load testing*, TRB, Washington, DC.